

# GMRT observations of the radio trail from CXOU J163802.6–471358

D. A. Green<sup>1</sup>★ and S. Roy<sup>2</sup>★

<sup>1</sup>*Astrophysics Group, Cavendish Laboratory, 19 J. J. Thomson Avenue, Cambridge CB3 0HE*

<sup>2</sup>*National Centre for Radio Astrophysics – Tata Institute of Fundamental Research, Pune, Pune University Campus, Post Bag 3, Ganeshkhind Pune 411007, INDIA*

Accepted —; received —; in original form —

## ABSTRACT

The X-ray source CXOU J163802.6–471358 is thought to be a pulsar wind nebula (PWN), as it shows an extended,  $\approx 40$  arcsec trail from a compact source. Here we present GMRT observations of this source at 330 and 1390 MHz, which reveal a remarkable linear radio trail  $\approx 90$  arcsec in extent. Although the radio trail points back to the supernova remnant (SNR) G338.1+0.4,  $\approx 50$  arcmin from CXOU J163802.6–471358, associating it with this remnant would require a very large velocity for the pulsar. There are no known galactic SNRs close to the PWN and radio trail. No pulsar has yet been identified in CXOU J163802.6–471358, but if one could be found, this would allow more quantitative studies of the PWN and radio trail to be made.

**Key words:** radio continuum: ISM – ISM: individual objects: CXOU J163802.6–471358, G338.1+0.4 – pulsars: general – ISM: supernova remnants

## 1 INTRODUCTION

Supernovae (SNe) can produce both extended supernova remnants (SNRs) and also pulsars in the case of core collapse ‘type II’ SNe. Pulsars dissipate most of their rotational energy through relativistic winds, and in some circumstances these winds can produce a luminous nebula around the pulsar which is known as a pulsar wind nebula (PWN, see Gaensler & Slane 2006 for a review). In some, younger cases the PWN dominates the SNR, e.g. Crab nebula (=G184.6–5.8) and 3C58 (=G130.7+3.1), see Bühler & Blandford (2014); Kothes (2013) and references therein. In other, old cases the pulsar/PWN is within the shell of the remnant, e.g. MSH 15-56 (=G326.3–1.8), see Dickel et al. (2000); Temim et al. (2017).

Some asymmetric SNe produce pulsars with large ‘kick’ velocity (e.g. Janka 2017; Holland-Ashford et al. 2017), and in cases where a pulsar is moving through the surrounding medium supersonically, then it forms a bow shock PWN due to ram pressure (e.g. Gaensler & Slane 2006). Such a PWN may be within the supernova remnant shell, or if the kick velocity or age are large enough, outside it. About sixty PWNs are known (Roberts 2004), with only about 15 PWNs are seen to have the morphology of a bow shock PWN, e.g. G270.3–1.0, the ‘Lighthouse nebula’ (=IGR J11014–6103) near the SNR G290.1–0.8 (=MSH 11–61A), G315.9–0.0 (= the ‘Frying Pan’), G341.2+0.9, G359.2–0.8 (= the ‘Mouse’, e.g. Hales et al. 2009), G5.27–0.9 (= the ‘Duck’), and G116.9+0.1 (=CTB 1, Schinzel et al. 2019; Kumar et al. 2023). Of these, the ‘Frying Pan’ (Camilo et al. 2009; Ng et al. 2012) is particularly striking, with a long radio trail extending  $\approx 8$  arcmin from the remnant shell, which has a radius of  $\approx 6$  arcmin. The extent of the radio trail is estimated to be about 20 pc, and the pulsar velocity about  $1000 \text{ km s}^{-1}$  for a distance of 8 kpc (but also see Wang et al. 2020 who give a lower distance for G315.9–0.0). Higher resolution radio images of this radio trail (Ng et al. 2012)

show that it has a ‘kink’, which reflects variations in the medium the pulsar is moving through. In the case of the ‘Lighthouse nebula’, X-ray observations (Pavan et al. 2016) show there is – in addition to a PWN trail about 1 arcmin long – there is also a curved ‘jet’ that is approximately perpendicular to the PWN trail. The ‘jet’ is fainter and longer than the PWN trail (at least 5 arcmin compared with PWN trail), and is well modelled by a helical geometry.

The X-ray source CXOU J163802.6–471358 (Fornasini et al. 2014; Jakobsen et al. 2014) is thought to be a PWN, as Chandra observations show a faint, diffuse ‘tail’  $\approx 40$  arcsec long extending to the north of a compact source. CXOU J163802.6–471358 has Galactic coordinates of  $l \approx 337^\circ.48$ ,  $b \approx -0^\circ.15$ , so lies very close to the Galactic plane. The number of Chandra counts in the ‘tail’ is small, only 110. Jakobsen et al. note also that there is a suggestion from smoothed images that there may be a shorter, fainter extension to west of the compact source – i.e. perpendicular to the main ‘tail’ – but the significance is of this is low ( $2.9\sigma$ ), given the small number of X-ray counts. Further, Jakobsen et al. note this source is also detected by XMM, and that there is a faint radio source in the Molonglo Galactic Plane Survey (MGPS-2, Murphy et al. 2007) survey at 843-MHz. The XMM source was subsequently catalogued as 3XMM J163802.6–471357 in the 3rd XMM–Newton serendipitous survey (Rosen et al. 2016). Jakobsen et al. describe the MGPS-2 radio source as being an unresolved, and offset from the compact X-ray source by about 40 arcsec. However, the resolution of the MGPS-2 image is rather low ( $43 \times 64 \text{ arcsec}^2$  elongated north–south). The MGPS-2 image also shows a possible faint extension  $\sim 3$  arcmin to the north, although there appear to be artefacts in the image, which is in a complex region of the Galactic plane. Subsequently CXOU J163802.6–471358 has also been detected in hard X-rays by NuSTAR (Fornasini et al. 2017). To date no pulsar has been detected within CXOU J163802.6–471358.

In order to clarify the nature of the faint MGPS radio source, we have obtained higher resolution radio observations of it, at both 322

★ email: dag@mrao.cam.ac.uk, roy@ncra.tifr.res.in

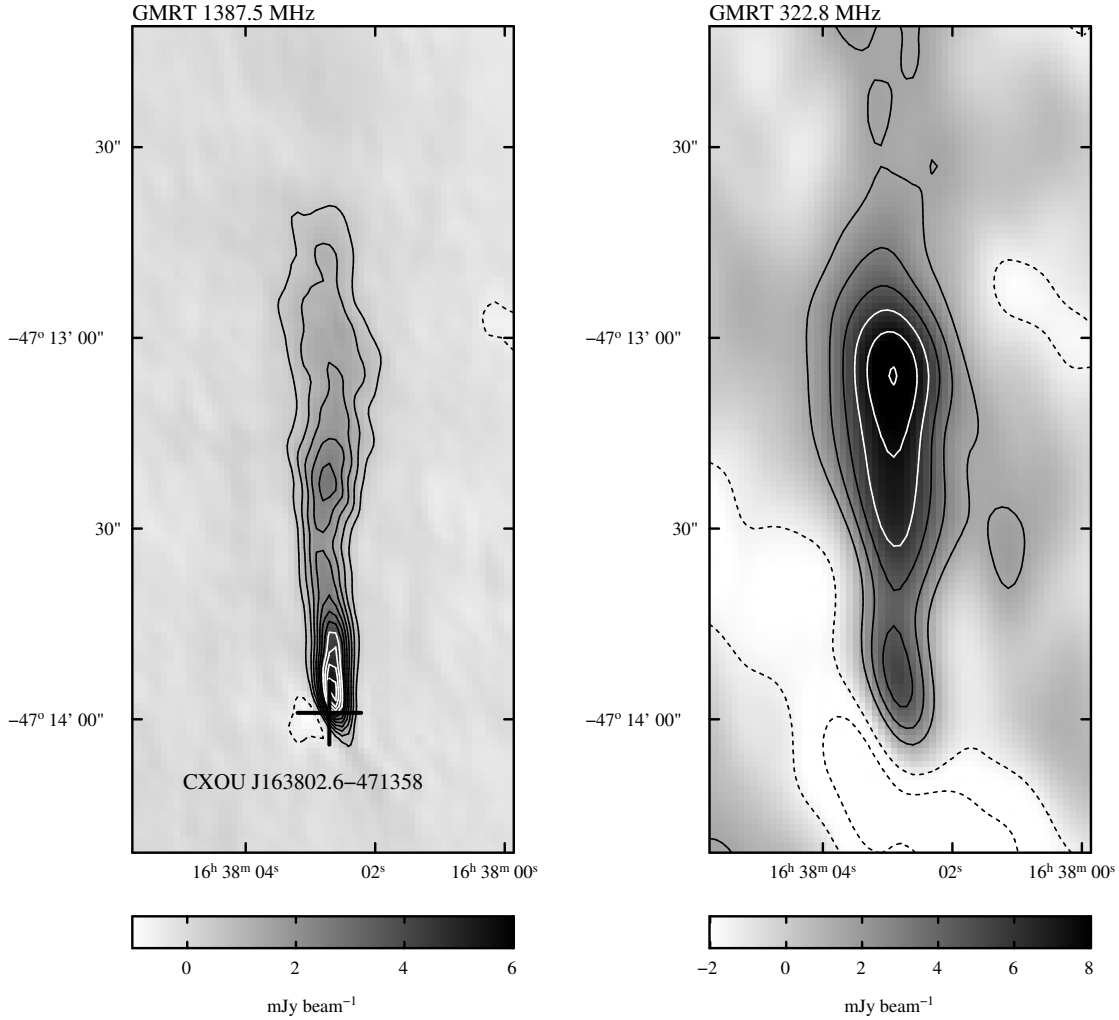


**Figure 1.** Image of radio trail from CXOU J163802.6–471358 at 1387.5 and 322.8 MHz from GMRT observations, in J2000.0 equatorial coordinates. At 1387.5 MHz the greyscale is  $-1$  to  $+6$   $\text{mJy beam}^{-1}$  with contours every  $0.5$   $\text{mJy beam}^{-1}$ , and the resolution is  $15.0 \times 6.1$   $\text{arcsec}^2$  at a position angle of  $8.9^\circ$  (E of N). At 322.8 MHz the greyscale is  $-2$  to  $+8$   $\text{mJy beam}^{-1}$  with contours every  $1.5$   $\text{mJy beam}^{-1}$ , and the resolution  $6.0 \times 3.1$   $\text{arcsec}^2$  at a position angle of  $24^\circ$ . Negative contours are dashed.

and 1390-MHz, with Giant Meterwave Radio Telescope (GMRT) which reveal it to be a remarkably long linear trail. Section 2 describes the observations and presents the resulting images. These are discussed in Section 3, and our conclusions presented in Section 4.

## 2 OBSERVATIONS AND RESULTS

The GMRT – see Pramesh Rao (2002) – is a synthesis telescope consisting of thirty 45-m antennas, that provides baselines up to  $\sim 25$  km. CXOU J163802.6–471358 was observed with the GMRT at both 330 and 1390 MHz, in separate observing sessions on 2015 July 9th and 23rd respectively. Each observation was made with a bandwidth of 32 MHz, divided into 256 channels. Since CXOU J163802.6–471358 is at a declination of  $\approx -47^\circ$  and the GMRT is at a latitude of  $\approx 19^\circ$ , these observations were made at low elevations ( $17^\circ$  to  $24^\circ$ ), with about 2.5 hours integration time on the source. Each observing session included a short observation of 3C286, which was used for flux density calibration, and interleaved observations of nearby secondary calibrators. The data was analysed following the standard procedures in AIPS (e.g. Greisen 2003).

Because CXOU J163802.6–471358 is at such a low declination, there was no known standard 330-MHz secondary calibrator within  $15$  deg of it. However, a compact, bright source J1627–3953 was identified from the NRAO VLA Sky Survey (NVSS, Condon et al. 1998) at 1.4 GHz, which was found to be compact and bright at 330 MHz with the GMRT, with a flux density of about 6 Jy. This was used as the secondary calibrator for the 330-MHz observations, with the model of the calibrator also including two much weaker sources in the field of view. J1627–3953 was observed approximately about every thirty minutes, and was also used as the bandpass calibrator at 330 MHz. After calibration and editing of the 330-MHz data, 10 adjacent frequency channels were averaged providing a channel width of 1.25 MHz in the output data. This reduces the data volume significantly, while keeping bandwidth smearing smaller than the synthesized beam during imaging up to half power point of primary beam of the GMRT. Imaging of CXOU J163802.6–471358 at 330 MHz is not straightforward, due to large field of view of the GMRT and the position of CXOU J163802.6–471358 in the Galactic plane near various sources of emission on a wide range of angular scales. Initial images were made, using multiple facets to cover the field of view (see Kogan & Greisen 2009), and improved by two

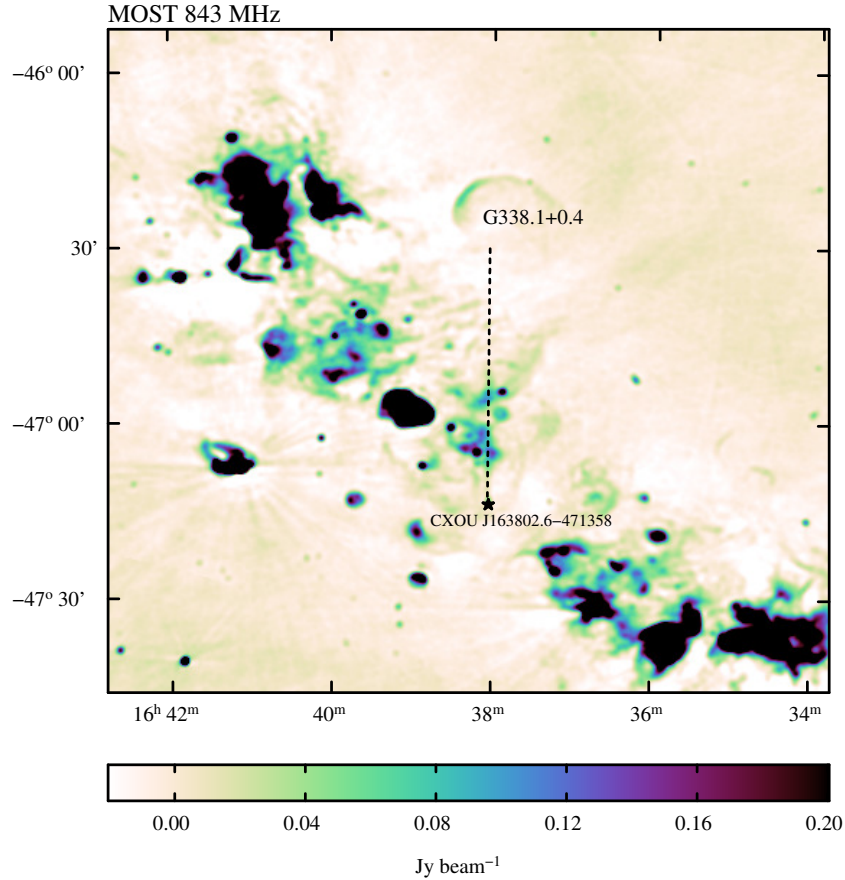


**Figure 2.** Molonglo Galactic Plane Survey (Murphy et al. 2007) observations, at 843 MHz of region surrounding CXOU J163802.6–471358, in J2000.0 equatorial coordinates. The resolution is  $45 \times 45 \text{ cosec}(|\text{Dec}|) \text{ arcsec}^2$ , and the ‘cubehelix’ colour scheme (Green 2011) is from  $-20$  to  $200 \text{ mJy beam}^{-1}$ . The position of CXOU J163802.6–471358 is marked with a star, and the dotted line show the alignment of the radio trail from it.

cycles of phase-only self-calibration. The final image was made in two steps.

(i) A high resolution CLEANed image of all the facets were made with a short  $uv$  cut-off of  $1 \text{ k}\lambda$ , to exclude extended emission of angular size  $\geq 3 \text{ arcmin}$ . All the significant CLEAN components produced in all the facets were then subtracted from the self-calibrated  $uv$  data.

(ii) A low resolution image from the resulting  $uv$ -data was then made with no  $uv$  cutoff, and significant CLEAN components from this image were then subtracted from  $uv$  data used in first step. Separating out the short spacings reduces the effect of the extended background Galactic emission. These data were then used to image the CXOU J163802.6–471358 for baselines  $> 0.8 \text{ k}\lambda$ .

In this processing some end channels were removed, as the ends of the bandpasses have poor responses, giving an effective bandwidth of  $28 \text{ MHz}$ , centred at  $322.8 \text{ MHz}$ . The resulting image of CXOU J163802.6–471358 is shown in Fig. 1. This has a resolution of  $15.0 \times 6.1 \text{ arcsec}^2$ , with an r.m.s. noise of  $\approx 1 \text{ mJy beam}^{-1}$ . As noted above, because CXOU J163802.6–471358 is in the Galactic plane, the local baselevel of the resulting image is not well defined.

At  $1390 \text{ MHz}$  the compact source J1626–2951 was observed approximately every 40 min, and was used as the secondary calibrator. The observations were calibrated using standard techniques. The observations of 3C286 were used to derive antenna based bandpass corrections. Several central channels were averaged together, and the observations of J1626–298 were used to calibrate the amplitude and

phase of the antennas through the observations. The derived antenna-based bandpass, and amplitude/phase calibrations were then applied to the observations of CXOU J163802.6–471358.

For the  $1390 \text{ MHz}$  observations 240 channels were retained, as the ends of the bandpasses have poor responses, giving an effective bandwidth of  $30 \text{ MHz}$ , centred at  $1387.5 \text{ MHz}$ . Adjacent groups of 10 channels were averaged together for imaging. Several cycle of self-calibration were applied, adjusting the phase only on timescales of 11, 5 and 1.5 min, and then one cycles of phase and amplitude self-calibration was applied, on a timescale of 1.5 min. The resulting image of CXOU J163802.6–471358 is shown in Fig. 1. This has a resolution of  $10.3 \times 5.3 \text{ arcsec}^2$ , with an r.m.s. noise of  $\approx 0.1 \text{ mJy beam}^{-1}$ .

### 3 DISCUSSION

These GMRT observations reveal a remarkably linear radio trail that extends  $\approx 90 \text{ arcsec}$  directly to the north of the X-ray compact source position, see Fig. 1. These results clearly show radio emission from the position of the compact X-ray source CXOU J163802.6–471358, with no offset (the ‘offset’ noted by Jakobsen et al. being due to the low resolution of the MGPS-2 radio image). The radio trail broadens and fades away from the position of CXOU J163802.6–471358. As noted above, there is a suggestion of a fainter X-ray trail perpendicular to the main trail from the compact X-ray source (cf. the ‘Lighthouse

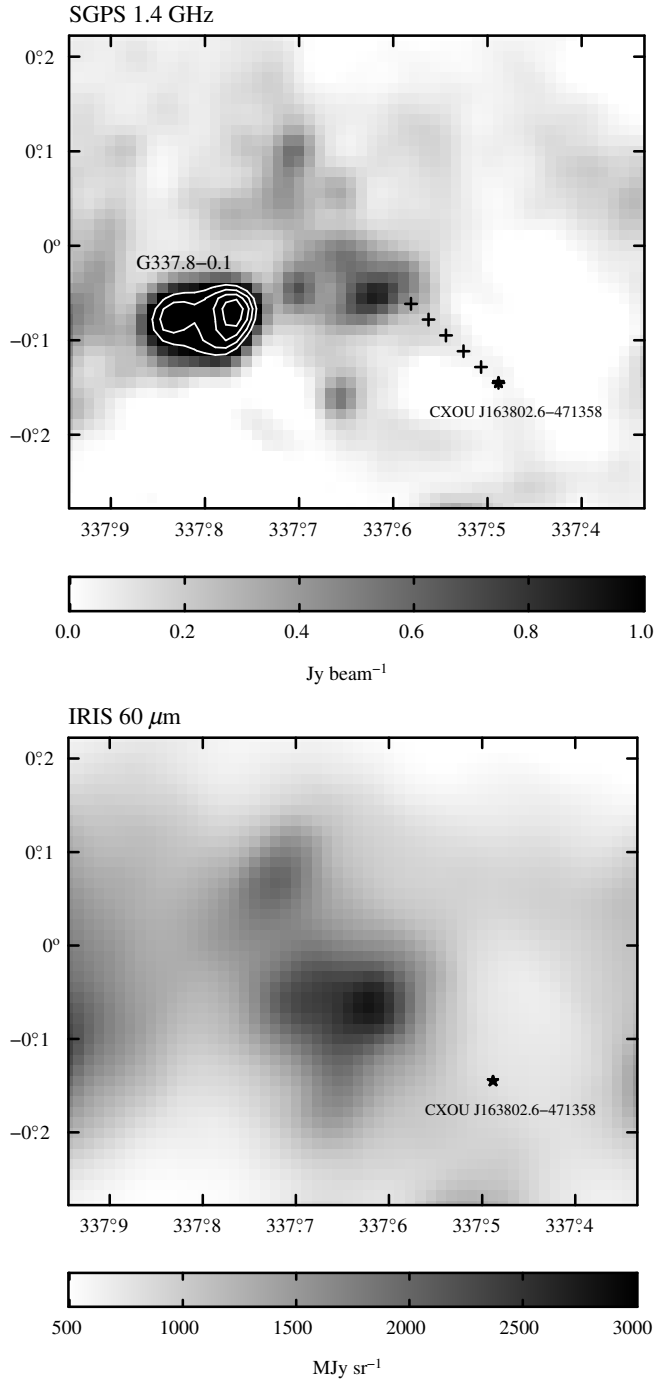


**Figure 3.** Radio and infra-red emission from the region to the north of CXOU J163802.6–471358, shown by a star, in Galactic coordinates. (top) SGPS 1.4-GHz radio emission, with resolution 100 arcsec (Haverkorn et al. 2006). The greyscale is 0.0 to 1.0 Jy beam<sup>-1</sup>, with selected contours at 1.1, 1.4, 1.7 and 2.0 Jy beam<sup>-1</sup> for the bright emission from the SNR G337.8–0.1. The crosses mark the extension of the observed radio trail from CXOU J163802.6–471358. (bottom) IRIS 60- $\mu$ m emission, with resolution of  $\approx 3$  arcmin (Miville-Deschênes & Lagache 2005). The greyscale is 500 to 3000 MJy sr<sup>-1</sup>.

nebula’), but there is no indication of any radio emission in a perpendicular direction. Determining the spectral index of the source is limited due to variations in the background emission near source in the lower frequency image. Its spectral index is consistent with being flat, but with a large uncertainty (about 0.4) in the spectral index.

Assuming that CXOU J163802.6–471358 contains a pulsar, and the radio trail is due to ram pressure stripping of the pulsar wind nebula moving supersonically through the ISM, then it would be expected that this pulsar originated in a SNR directly to the north of the radio trail. There are no catalogued Galactic SNRs nearby, i.e. within a few tens of arcmin, to the north of the radio trail. The closest known SNR is G337.8–0.1 near  $16^{\text{h}}39^{\text{m}}, -47^{\circ}$  (e.g. Shaver & Goss 1970; Whiteoak & Green 1996), which is thought most likely to be in the Norma II arm, at a distance of about 11 kpc (Kothes & Dougherty 2007). However, this is not aligned with the direction of the radio trail, but is misaligned by about 30 deg.

There is a catalogued remnant – G338.1+0.4, near  $16^{\text{h}}38^{\text{m}}, -46^{\circ}25'$  (e.g. Shaver & Goss 1970; Zealey et al. 1979; Whiteoak & Green 1996) – that does lie due north of CXOU J163802.6–471358, i.e. along the line traced by the radio trail, but this is quite far away. G338.1+0.4 is a slightly elongated shell remnant,  $\approx 16 \times 14$  arcmin<sup>2</sup> in extent at radio wavelengths (e.g. Whiteoak & Green 1996), and has been detected optically (Zealey et al. 1979). Fig. 2 shows radio image of the region of the Galactic plane from the Molonglo Galactic Plane Survey (MGPS-2, see Murphy et al. 2007) near CXOU J163802.6–471358, including G338.1+0.4. The centroid of G338.1+0.4 is  $l \approx 338^{\circ}05', b \approx 0^{\circ}45'$ , which is about  $\sim 0^{\circ}8'$  from CXOU J163802.6–471358, i.e. about 7 times the radius of G338.1+0.4. Hence, if CXOU J163802.6–471358 was born by the supernova that produced G338.1+0.4, then the velocity of pulsar in the plane of the sky would have to be 7 times the average expansion velocity of the remnant. No direct distance measurement is available for G338.1+0.4, but the fact that it is visible optically suggests that it is not very distant. If G338.1+0.4 is at 5 kpc, would have a radius of  $\approx 12$  pc, and for a nominal SN energy of  $10^{44}$  J and an ISM density of  $1 \text{ cm}^{-3}$ , a Sedov evolution model for the remnant would imply an age of about 8000 yr and an average expansion velocity of about  $1400 \text{ km s}^{-1}$ . This would require an extremely large pulsar transverse (i.e. in the plane of the sky) velocity of  $9800 \text{ km s}^{-1}$ . This is much larger than the highest pulsar velocities known, e.g. Chatterjee et al. (2005), who measure a transverse velocity of  $1083^{+103}_{-90} \text{ km s}^{-1}$  for the pulsar B1508+55 from parallax and proper motion observations. In the case of the ‘Lighthouse nebula’, higher velocities of 2400–2900  $\text{km s}^{-1}$  have been suggested for IGR J11014–6103 (Tomsick et al. 2012), depending on the distance and age of the remnant G290.1–0.8. More recently (Pavan et al. 2016) use a somewhat a smaller distance to the remnant, but still derive a large pulsar velocity of  $\approx 1000 \text{ km s}^{-1}$ ). Also, a velocity as large as  $9800 \text{ km s}^{-1}$  is not possible to reconcile with a standard SN explosion, since the kinetic energy of a  $1.5 M_{\odot}$  neutron star moving at  $9800 \text{ km s}^{-1}$  is  $\approx 1.4 \times 10^{44}$  J, which is comparable with the nominal total SN energy.

Thus, the pulsar and CXOU J163802.6–471358 must have been born in a different SNR than G338.1+0.4. The MGPS-2 image in Fig. 2 show a complex region of radio features near  $16^{\text{h}}38^{\text{m}}15^{\text{s}}, +47^{\circ}3'$  (or  $l \approx 337^{\circ}65', b \approx -0^{\circ}05'$ ) which lie to the north of CXOU J163802.6–471358, much closer than G338.1+0.4 to the radio trail. However, there are no catalogued SNRs in this region (Green 2019), nor are there any reported SNR candidates (see Section 2.3 of Green 2022). Fig. 3 shows SGPS (see Haverkorn et al. 2006) radio and IRIS (see Miville-Deschênes & Lagache 2005) 60  $\mu$ m infra-red images of this region. These show that the radio emitting features, apart from G337.8–0.1, are all associated with infra-red emission. Indeed in the

WISE H II region catalogue (Anderson et al. 2014) includes several known, candidate and ‘radio quiet’ H II regions near  $l = 337^{\circ}.65$ ,  $b = -0^{\circ}.05$ . These include G337.665–0.048 listed in (Caswell & Haynes 1987), and an ultracompact H II region G337.6156–0.0606 identified from IRAS observations (Walsh et al. 1997, 1998). Thus it is likely that the parent SNR of CXOU J163802.6–471358 is so old, and hence faint at radio wavelengths that it is not identifiable. For an age of  $10^5$  yr, and pulsar speed of  $\sim 200 \text{ km s}^{-1}$  in the plane of the sky (e.g. Igoshev 2020), this corresponds to a linear distance of 21 pc (or 14 arcmin at 5 kpc).

As yet no pulsar has yet been directly identified in CXOU J163802.6–471358, which means that no direct proper motion is available, nor is a distance estimate from the pulsar dispersion measure. Identification of the presumed pulsar in CXOU J163802.6–471358 is needed for better understanding of any associated parent SNR.

#### 4 CONCLUSIONS

GMRT observations of the X-ray source CXOU J163802.6–471358, which is thought to be a PWN, at 330 and 1390 MHz, reveal a remarkable linear radio trail extending  $\approx 90$  arcsec to the north. Such a PWN trail is expected to point back to the supernova remnant that produced the pulsar. The closest known SNR to CXOU J163802.6–471358 is G337.8–0.1, but this is misaligned with the radio trail by about 30 deg. There is a known SNR, G338.1+0.4, which is aligned with the radio trail. But it is  $\approx 50$  arcmin from CXOU J163802.6–471358, which would require a very high pulsar transverse velocity for it to be where the pulsar in CXOU J163802.6–471358 to have been born. Thus, the parent SNR of this PWN is not currently identified. Clearly, an identification of a pulsar would allow more quantitative studies of the PWN and radio trail to be made.

#### ACKNOWLEDGEMENTS

We thank the staff of the GMRT who have made these observations possible. The GMRT is run by the National Centre for Radio Astrophysics of the Tata Institute of Fundamental Research. We also thank the NCRA Director for the allocation of discretionary time on the GMRT, and DAG thanks NCRA for their hospitality during a sabbatical visit, when this study was initiated.

#### DATA AVAILABILITY

The GMRT data underlying this article are available from the GMRT Online Archive (<https://naps.ncra.tifr.res.in/goa/>) for ProposalID ddtB173. The other data use in Figs. 2 and 3 are available from <http://www.astrop.physics.usyd.edu.au/mosaics/Galactic/>, [https://www.atnf.csiro.au/research/HI/sgps/fits\\_files.html](https://www.atnf.csiro.au/research/HI/sgps/fits_files.html) and <https://irsa.ipac.caltech.edu/data/IRIS/images/>.

#### References

Anderson L. D., Bania T. M., Balser D. S., Cunningham V., Wenger T. V., Johnstone B. M., Armentrout W. P., 2014, *ApJS*, 212, 1  
 Bühler R., Blandford R., 2014, *Rep. Prog. Phys.*, 77, 066901  
 Camilo F., Ng C.-Y., Gaensler B. M., Ransom S. M., Chatterjee S., Reynolds J., Sarkissian J., 2009, *ApJ*, 703, L55

Caswell J. L., Haynes R. F., 1987, *A&A*, 171, 261  
 Chatterjee S., et al., 2005, *ApJ*, 630, L61  
 Condon J. J., Cotton W. D., Greisen E. W., Yin Q. F., Perley R. A., Taylor G. B., Broderick J. J., 1998, *AJ*, 115, 1693  
 Dickel J. R., Milne D. K., Strom R. G., 2000, *ApJ*, 543, 840  
 Fornasini F. M., et al., 2014, *ApJ*, 796, 105  
 Fornasini F. M., et al., 2017, *ApJS*, 229, 33  
 Gaensler B. M., Slane P. O., 2006, *ARA&A*, 44, 17  
 Green D. A., 2011, *Bull. Astron. Soc. India*, 39, 289  
 Green D. A., 2019, *J. Astrophys. Astron.*, 40, 36  
 Green D. A., 2022, ‘A Catalogue of Galactic Supernova Remnants’, <https://www.mrao.cam.ac.uk/surveys/snrns/>  
 Greisen E. W., 2003, in Heck A., ed., *Astrophysics and Space Science Library*, Vol. 285, *Information Handling in Astronomy – Historical Vistas*. Kluwer Academic Publishers, Dordrecht, p. 109  
 Hales C. A., Gaensler B. M., Chatterjee S., van der Swaluw E., Camilo F., 2009, *ApJ*, 706, 1316  
 Haverkorn M., Gaensler B. M., McClure-Griffiths N. M., Dickey J. M., Green A. J., 2006, *ApJS*, 167, 230  
 Holland-Ashford T., Lopez L. A., Auchettl K., Temim T., Ramirez-Ruiz E., 2017, *ApJ*, 844, 84  
 Igoshev A. P., 2020, *MNRAS*, 494, 3663  
 Jakobsen S. J., Tomsick J. A., Watson D., Gotthelf E. V., Kaspi V. M., 2014, *ApJ*, 787, 129  
 Janka H.-T., 2017, *ApJ*, 837, 84  
 Kogan, L., Greisen, E. W., 2009, ‘Faceted imaging in AIPS’ (AIPS Memo 113), <http://www.aips.nrao.edu/TEXT/PUBL/AIPSMEM113.PS>  
 Kothes R., 2013, *A&A*, 560, A18  
 Kothes R., Dougherty S. M., 2007, *A&A*, 468, 993  
 Kumar P., Schinzel F. K., Taylor G. B., Kerr M., Castro D., Rau U., Bhatnagar S., 2023, *ApJ*, 945, 129  
 Miville-Deschênes M.-A., Lagache G., 2005, *ApJS*, 157, 302  
 Murphy T., Mauch T., Green A., Hunstead R. W., Piestrzynska B., Kels A. P., Sztajer P., 2007, *MNRAS*, 382, 382  
 Ng C.-Y., Bucciantini N., Gaensler B. M., Camilo F., Chatterjee S., Bouchard A., 2012, *ApJ*, 746, 105  
 Pavan L., et al., 2016, *A&A*, 591, A91  
 Pramesh Rao A., 2002, in: A. Pramesh Rao, G. Swarup & Gopal-Krishna (eds), *The Universe at Low Radio Frequencies*, Proc. IAU Symposium No. 199, (San Francisco: ASP), p. 439  
 Roberts, M.S.E., 2004, ‘The Pulsar Wind Nebula Catalog (March 2005 version)’, McGill University, Montreal, Quebec, Canada (available on the World-Wide-Web at <http://www.physics.mcgill.ca/~pulsar/pwnecat.html>).  
 Rosen S. R., et al., 2016, *A&A*, 590, A1  
 Schinzel F. K., Kerr M., Rau U., Bhatnagar S., Frail D. A., 2019, *ApJ*, 876, L17  
 Shaver P. A., Goss W. M., 1970, *Aust. J. Phys. Suppl.*, 14, 133  
 Temim T., Slane P., Plucinsky P. P., Gelfand J., Castro D., Kolb C., 2017, *ApJ*, 851, 128  
 Tomsick J. A., Bodaghee A., Rodriguez J., Chaty S., Camilo F., Fornasini F., Rahoui F., 2012, *ApJ*, 750, L39  
 Walsh A. J., Hyland A. R., Robinson G., Burton M. G., 1997, *MNRAS*, 291, 261  
 Walsh A. J., Burton M. G., Hyland A. R., Robinson G., 1998, *MNRAS*, 301, 640  
 Wang S., Zhang C., Jiang B., Zhao H., Chen B., Chen X., Gao J., Liu J., 2020, *A&A*, 639, A72  
 Whiteoak J. B. Z., Green A. J., 1996, *A&AS*, 118, 329  
 Zealey W. J., Elliott K. H., Malin D. F., 1979, *A&AS*, 38, 39

This paper has been typeset from a  $\text{\TeX}/\text{\LaTeX}$  file prepared by the author.